

Thermodynamic Performance and Lifetime Prediction Model of High-Voltage Transmission Lines in High Temperature and High Humidity Environments



Wei Cui 

Guangdong Electric Power Design Institute Co., Ltd of China Energy Engineering Roup, Guangzhou 510700, China

Corresponding Author Email: cuiwei@gedi.com.cn

Copyright: ©2024 The author. This article is published by IIETA and is licensed under the CC BY 4.0 license (<http://creativecommons.org/licenses/by/4.0/>).

<https://doi.org/10.18280/ijht.420625>

ABSTRACT

Received: 17 June 2024

Revised: 22 October 2024

Accepted: 7 November 2024

Available online: 31 December 2024

Keywords:

high-temperature and high-humidity environment, high-voltage transmission line, thermal stress, fatigue life, thermodynamic analysis, lifetime prediction

With the intensification of global climate change, extreme weather events are becoming more frequent, and the thermodynamic performance and fatigue life of high-voltage transmission lines in high-temperature and high-humidity environments are increasingly drawing attention. High-temperature and high-humidity conditions have a complex impact on the thermal stress and material fatigue of transmission lines, potentially reducing the reliability and service life of the power grid. To address this issue, this paper proposes a thermodynamic analysis-based model for calculating thermal stress and predicting fatigue life of high-voltage transmission lines under high-temperature and high-humidity conditions. The study first provides a detailed analysis of the thermal stress in transmission lines under high-temperature and high-humidity conditions, revealing the impact of temperature and humidity variations on the thermal expansion and deformation of the lines. Subsequently, combining material fatigue theory, the paper establishes a fatigue life prediction model for the lines, quantifying the accumulation process of fatigue damage under the influence of thermal stress. Through this theoretical model, the paper aims to provide a scientific basis for the design, evaluation, and maintenance of high-voltage transmission lines in harsh environments, ensuring the stability and safety of the power system.

1. INTRODUCTION

With the continuous growth of energy demand in modern society, high-voltage transmission lines, as an important component of power transmission, have become increasingly critical in terms of their safety and stability [1-6]. In high-temperature and high-humidity environmental conditions, especially in the context of climate change and frequent extreme weather events, the thermodynamic loads and long-term fatigue that transmission lines endure may significantly impact their performance and service life. High-temperature and high-humidity environments not only lead to thermal expansion and deformation of the lines but also exacerbate the fatigue damage of the line materials, thus affecting the reliability and economy of the transmission system [7-9]. Therefore, studying the thermodynamic performance and lifetime prediction of high-voltage transmission lines in such environments is of great practical significance and application value.

Researching the thermodynamic behavior and fatigue life of high-voltage transmission lines under extreme climate conditions not only helps improve the design and maintenance levels of transmission lines but also provides a theoretical basis for the reliability assessment of power systems [10-14]. During prolonged operation, the accumulation of thermal stress in the lines and the accumulation of material fatigue can lead to aging, and even fracture or failure of the lines, thus

affecting the safety of power supply [15, 16]. Therefore, accurately predicting the thermal stress changes and fatigue life of the lines in high-temperature and high-humidity environments is crucial for precise maintenance, early warning, and optimized design of high-voltage transmission lines.

Currently, research on transmission lines in high-temperature and high-humidity environments mainly focuses on the analysis of single-factor influences [17-23], and most studies lack a comprehensive assessment of thermal stress and fatigue life. Existing research methods often rely on empirical formulas or simplified assumptions, ignoring the complexity and multivariable interactions in real-world environments. In addition, current fatigue life prediction models often fail to fully consider the dynamic impact of temperature and humidity changes on the long-term performance of the lines, resulting in poor accuracy and reliability of the prediction results. Therefore, how to combine the evolution process of thermal stress and fatigue damage to propose a more precise and systematic analysis method remains an urgent problem to solve.

The main research content of this paper is divided into two parts. First, focusing on the thermal stress calculation and analysis of high-voltage transmission lines in high-temperature and high-humidity environments, this paper will accurately describe the thermal expansion behavior of the lines under different temperature and humidity conditions through thermodynamic models and conduct stress analysis to reveal

the impact of environmental factors on the thermal stress of the lines. Secondly, based on the thermodynamic analysis results and combined with the material's fatigue performance, this paper will construct a fatigue life prediction model for high-voltage transmission lines under high-temperature and high-humidity conditions. Through these two parts of research, this paper aims to provide theoretical support for the reliability assessment of high-voltage transmission lines in harsh environments and provide a scientific basis for the optimization design and management of transmission lines, thereby improving the stability and safety of the power system.

2. THERMAL STRESS CALCULATION AND ANALYSIS OF HIGH-VOLTAGE TRANSMISSION LINES IN HIGH TEMPERATURE AND HIGH HUMIDITY ENVIRONMENTS

Figure 1 shows the schematic diagram of the thermal process of the cross-section of a high-voltage transmission line. In high-temperature and high-humidity environments, the external thermal loads and mechanical tension acting on the high-voltage transmission lines cause thermal expansion, which in turn generates thermal stress between the layers of conductors. To accurately calculate the thermal stress of the line under such environmental conditions, this paper fully considers the complexity of the line structure, especially the relative movement between layers and the differences in thermal expansion, and adopts a layered thermal stress calculation method. This method can more accurately reflect the distribution of thermal stress within the line. In the specific calculation process, the following assumptions must be clarified, as they help simplify the model while ensuring the rationality and operability of the calculation results.

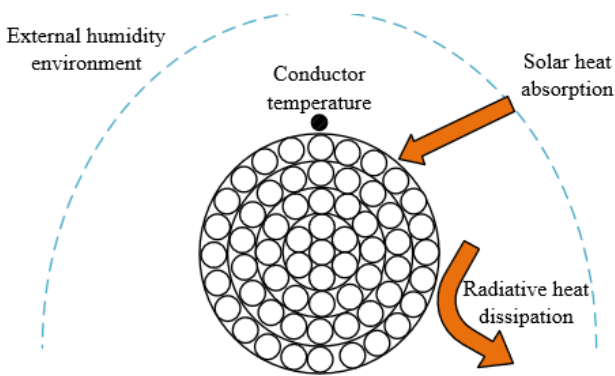


Figure 1. Schematic diagram of the thermal process of the cross-section of a high-voltage transmission line

Assumption 1: The conductors in the same layer are in the same stress state

It is assumed that in each layer of the line conductors, the forces and stresses are uniformly distributed among all the conductors. Figure 2 shows the schematic diagram of the cross-section of a high-voltage transmission line. Since the conductors in each layer are wound in a helical structure, it is assumed that the stress state is the same for all conductors in each layer, and the conductor axes lie on the same cylindrical surface. This assumption is made to avoid considering the tiny differences between each conductor during the calculation, thereby simplifying the analysis model and making the thermal stress calculation more intuitive and operable. With

this assumption, it can be assumed that the thermal expansion and forces are uniform for the conductors in each layer, facilitating the layered calculation of thermal stress.

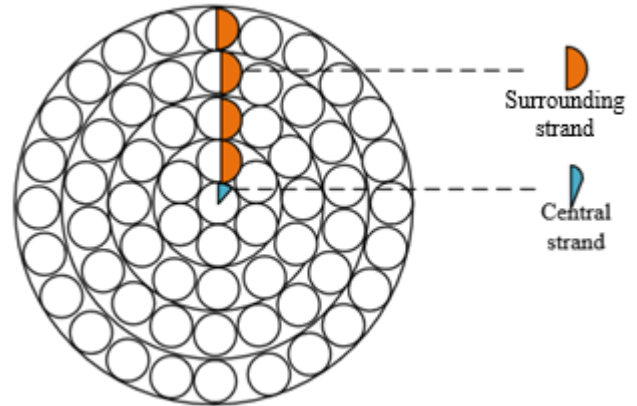


Figure 2. Schematic diagram of the cross-section of a high-voltage transmission line

Assumption 2: The change in the helical angle of conductors in the same layer is small

Since the conductors in each layer of a high-voltage transmission line are twisted at a certain helical angle, the size of the helical angle affects the relative position and force of each conductor. Under high-temperature and high-humidity environments, the expansion and tension of the conductor materials may cause some changes in the helical angle. However, to simplify the model analysis, it is assumed that the change in the helical angle of conductors in each layer is small and remains basically unchanged. This allows for ignoring the dynamic change of the helical angle in the calculation and considering only the initial design angle. Through this assumption, the calculation complexity is effectively reduced, avoiding the impact of complex geometric changes caused by the variation in helical angles on the thermal stress calculation.

Assumption 3: No frictional force between layers

In actual high-voltage transmission lines, the conductors in different layers may experience relative sliding and friction due to the operational tension. However, due to the significant effect of thermal expansion in high-temperature and high-humidity environments, and because the frictional force is usually small, the effect of inter-layer frictional forces on the thermal stress of the conductor can be ignored. Through this assumption, the additional thermal stress caused by friction between layers does not need to be considered in the calculation, and the thermal stress is calculated based on the effects of thermal expansion and tension.

The twist angle α_v is the angle formed between the direction of the conductor strands and the axis during the winding of the strands around the core wire. The twist angle directly affects the spatial helical shape of the conductors in each layer. To calculate the thermal stress, it is necessary to first determine the twist angle and pitch of each layer of conductors. The pitch refers to the height the conductor climbs along the axis when it wraps around the core wire in one turn. The diameter f of each conductor strand and the outer diameter F_v are closely related to the twist angle and pitch. The size of the twist angle determines the helical shape of the conductor strands, which in turn affects the force and deformation of each layer of conductors. Therefore, it is first necessary to determine the twist angle and pitch based on the geometric parameters of the

conductor to provide the basic data for subsequent thermal stress calculations. The specific calculation formulas are:

$$\tan \alpha_v = \frac{\pi(F_v - f)}{M} \quad (1)$$

Since the structure and physical properties of the conductors in each layer of the wire are different, the mechanical properties (such as elastic modulus, tensile strength, etc.) and stress state of each layer of conductors will also vary. In high-temperature and high-humidity environments, temperature changes cause thermal expansion of the conductor material, resulting in thermal stress. Meanwhile, the conductor also bears external tension during operation. These factors together lead to a complex variation in the stress distribution across each layer of conductors. Therefore, the second step is to analyze the mechanical properties and stress state of each layer of conductors in detail, including the elongation of each layer of conductors and their deformation under temperature changes and operational tension. Let the elongation of the ν -th layer of conductor be denoted by ΔM_ν , the elongation of the ν -th layer after elongation by m'_ν , and the initial length of the ν -th layer before elongation by m_ν . The elongation of the conductor strand is:

$$\Delta M_\nu = m'_\nu - m_\nu \quad (2)$$

In high-temperature and high-humidity environments, each layer of conductor will experience thermal expansion due to temperature changes. There is a certain relationship between the elongation of each layer of conductor and the total elongation of the conductor. The elongation of the conductor strand depends on its material's coefficient of thermal expansion, the temperature change, and the initial length of the strand. Since the conductor consists of multiple layers of strands, the elongation of each layer of conductor differs, so it is necessary to calculate the elongation of each layer separately and then determine the total elongation of the entire conductor through spatial geometric relations. In this process, the helical shape of the strands and the mutual constraints between them must be considered to ensure that the total elongation of the conductor accurately reflects the deformation of each layer of strand. The relationship between the elongation of the strand and the total elongation of the conductor is:

$$\Delta M_\nu = \Delta M \cos \alpha_v \quad (3)$$

Let the axial elongation rate of the conductor be denoted by γ , and the elongation rate of the ν -th layer of strand by γ_ν , which is:

$$\gamma_\nu = \gamma \cos \alpha_v \quad (4)$$

When the conductor is in a high-temperature and high-humidity environment, each layer of conductor is affected not only by temperature changes but also by tension. To calculate the thermal stress in each layer of conductor, it is necessary to apply the principles of material mechanics and consider the stress distribution due to elastic stretching. Based on the elongation of each layer of strand and the mechanical properties of the material, elastic theory can be used to calculate the stress state of the strand. Special attention must

be paid to the effect of high temperatures on material properties, as high temperatures cause changes in the elastic modulus of the material, which in turn affects the stress calculation results. The stress value in each layer of conductor will vary with temperature changes and tension, so a layer-by-layer analysis is required to obtain the layered thermal stress distribution. Let the elastic modulus of the ν -th layer of strand be denoted by R_ν , then when the conductor undergoes only elastic stretching, the stress δ'_ν of that layer is:

$$\delta'_\nu = \gamma R \cos^3 \alpha_v \quad (5)$$

When the conductor is subjected to both temperature and operational tension, part of the deformation is caused by temperature changes. The deformation caused by temperature changes and the deformation caused by tension are independent of each other. Therefore, in calculating the stress of the conductor strand, the deformation caused by temperature changes must be excluded. To do this, it is necessary to first determine the deformation caused by the temperature change in each layer of strand and remove it from the total deformation. The remaining deformation can then reflect the stress state caused by operational tension. At this point, let the coefficient of the strand in the ν -th layer be denoted by β_ν , the temperature change in the ν -th layer by Δs_ν , and the stress of the ν -th layer of strand is:

$$\delta'_\nu = R(\gamma \cos^3 \alpha_v - \beta_\nu \Delta s_\nu) \quad (6)$$

After removing the effect of temperature-induced deformation, the next step is to calculate the axial stress of each layer of conductor. Axial stress refers to the stress along the axial direction of the conductor strands, which is related not only to changes in temperature and tension but also to the mechanical properties of the conductor material. Specifically, this paper considers the elongation and stress state of each layer of strand and calculates the axial stress of each layer of conductor based on the basic principles of material mechanics. The formula for calculating the axial stress of the ν -th layer of conductor strand is:

$$\delta_\nu = R_\nu(\gamma \cos^3 \alpha_v - \beta_\nu \Delta s_\nu \cos \alpha_v) \quad (7)$$

Let the cross-sectional area of the layer of strand be denoted by X_ν , and the axial tension d_ν of the layer of strand is:

$$D_\nu = \delta_\nu X_\nu \quad (8)$$

Furthermore, assume that no plastic deformation occurs in the steel core and aluminum-stranded wires after stretching, and the effects of friction and Poisson's ratio are ignored. The total axial stress of each layer of conductor can be obtained through simple mechanical assumptions. This assumption greatly simplifies the calculation process, but it should be noted that it applies only to cases where only elastic deformation is considered, meaning that the deformation of the conductor under tension will not exceed the elastic limit. In this step, the axial stress of each layer of strand will be summed to obtain the total axial stress D of the entire conductor under specific temperature and tension. Let the diameter of the ν -th layer of strand be denoted by $d_{\nu f}$, and the number of strands in the ν -th layer by c_ν . The specific

calculation formula is:

$$D = \sum_{v=1}^s 250\pi(\gamma \cos^3 \alpha_v - \beta_v \Delta s_v \cos \alpha_v) R_v c_v f_v^2 \quad (9)$$

Once the temperature change and stress distribution of the strands are determined, the overall strain of the entire conductor can be further solved. The overall strain γ refers to the overall deformation of the conductor under the combined effect of temperature and tension. It is closely related to the physical properties of the conductor, temperature changes, and external tension. Once the overall strain is determined, the stress-strain relationship can be used to calculate the axial stress of the steel core and aluminum-stranded layers.

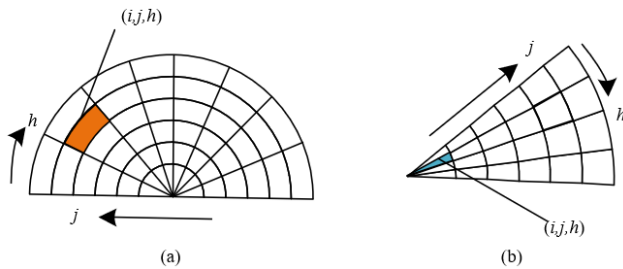


Figure 3. Finite element distribution of high voltage transmission conductor (a) surrounding strand; (b) central strand

In high-temperature and high-humidity environments, the analysis of the thermal stress and thermal strain distribution of high-voltage transmission conductors is a complex process, involving the comprehensive consideration of the conductor's geometric characteristics, material properties, environmental temperature, humidity, and other factors. To accurately predict the behavior of the conductor in such environments, modern engineering simulation technologies, such as three-dimensional modeling and finite element analysis tools, need to be used to analyze the thermal stress and thermal strain distribution of the conductor. Figure 3 shows the finite element distribution diagram of the high-voltage transmission conductor. The specific analysis steps are as follows:

Step 1: Establish the Three-Dimensional Model of the Conductor and Perform Mesh Division

First, a three-dimensional solid model of the conductor needs to be established using 3D modeling software ProE. The model should include the structural features of the conductor, the geometric parameters of each layer of strand, and the arrangement of the core wire and outer strands. When constructing the model, the specific material properties of the conductor, the structural characteristics of each strand layer, and important parameters such as the outer diameter of the conductor and the core wire diameter should be considered. After completing the 3D modeling, the model is imported into finite element analysis software ANSYS for mesh division. During the meshing process, appropriate mesh size and type should be selected based on the conductor's complex geometric shape and analysis requirements, ensuring the accuracy of the model and the reliability of the calculation results. The mesh division should be verified to ensure the convergence and accuracy of the simulation results.

Step 2: Use Axial Tension Calculation Method to Analyze Stress and Strain Distribution of the Conductor

In the finite element analysis software, based on the conductor's axial tension calculation method, a preliminary analysis of the stress and strain distribution of the conductor is conducted. In this step, the changes in stress and strain, especially the deformation and stress distribution caused by temperature, under high-temperature and high-humidity environments need to be considered. Figure 4 shows the schematic diagram of the temperature monitoring point distribution on the high-voltage transmission conductor. By applying axial tension, the deformation process of the conductor under stretching conditions is simulated, and the stress and strain state of each strand layer is calculated. When performing stress analysis, special attention should be paid to the mechanical performance differences of each strand layer, such as the stress state of different materials, and the temperature gradient changes should be considered to obtain the stress and strain distribution of each layer of the conductor.

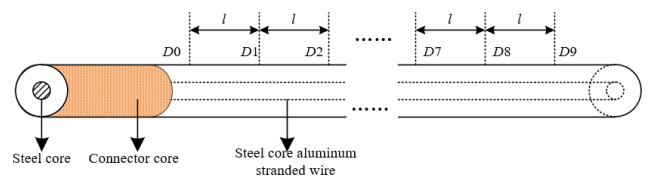


Figure 4. Temperature monitoring point distribution on high voltage transmission conductor

Step 3: Set Boundary Conditions and Analyze the Impact of Radial Temperature on Stress Distribution

In a high-temperature and high-humidity environment, the conductor will be affected by temperature changes, especially the radial temperature changes, which will cause different thermal expansion effects on each layer of conductor strands. In this phase, corresponding boundary conditions should be set in the finite element analysis model to simulate the actual situation of the conductor affected by environmental temperature changes. By setting different temperature distributions, the impact of radial temperature on the thermal stress distribution of each strand layer in the conductor is analyzed. The key to this step is accurately simulating the impact of temperature changes on each strand layer, especially the temperature gradient between the surface of the conductor and the core wire. This gradient difference will cause different expansion degrees in each layer of strands, which in turn affects the overall stress and strain distribution of the conductor.

Step 4: Consider the Impact of Radial Temperature and Calculate the Stress at the Suspension Points of the Conductor

In a high-temperature and high-humidity environment, the suspension points of the conductor are usually the places where stress concentration is most severe. To accurately calculate the stress at the suspension points, a parabolic approximation equation is typically used to simulate the suspension shape of the conductor. In this process, the radial temperature of the conductor is crucial to the stress at the suspension point, because temperature changes not only alter the length of the conductor but also affect the local stress state of the strands near the suspension point. By calculating the stress at the suspension points of the conductor, stress concentration areas that may occur during actual operation can be predicted, and corresponding engineering measures can be taken to avoid excessive stress concentration, thus ensuring the safe and stable operation of the conductor.

3. FATIGUE LIFE CALCULATION OF HIGH VOLTAGE TRANSMISSION CONDUCTOR IN HIGH TEMPERATURE AND HIGH HUMIDITY ENVIRONMENT

In a high temperature and high humidity environment, the fatigue life calculation of high voltage transmission conductors is a complex and critical engineering issue. During long-term operation, the conductor is affected by various environmental factors, such as wind speed, wind direction, temperature variations, and humidity. These factors cause stress fluctuations and fatigue damage to the conductor. To accurately predict the fatigue life of the conductor under such harsh environmental conditions, this paper uses a fatigue life calculation method based on wind speed and wind direction probability distribution, and combines Miner's cumulative damage theory to quantify the fatigue damage of the conductor. The calculation principles for fatigue life of the high voltage transmission conductor in high temperature and high humidity environment are detailed below.

3.1 Probability distribution analysis based on wind speed and wind direction

The fatigue life of the conductor is not only related to the mechanical properties of the material but is also significantly influenced by external environmental factors, especially wind speed and wind direction. In high temperature and high humidity environments, changes in wind speed and wind direction cause alternating stresses in the conductor during operation. These alternating stresses are the main factors leading to fatigue damage. Therefore, it is first necessary to analyze the variation patterns of wind speed and wind direction through probability distribution methods. In practical applications, wind speed and wind direction usually exhibit certain randomness, which can be simulated by collecting and analyzing local meteorological data, using appropriate probability distribution models to simulate stress fluctuations of the conductor under different wind speed and wind direction conditions.

The variation in wind speed causes the conductor to sway or vibrate, thereby generating alternating stresses. The variation in wind direction affects the direction and magnitude of the force on the conductor, so the combined effects of wind speed and wind direction must be considered. By modeling the probability distribution of wind speed and wind direction, this paper calculates the alternating stress amplitude and stress frequency of the conductor under different wind speed and wind direction conditions, providing the basic data for the subsequent fatigue life analysis.

3.2 Fatigue criteria and life assessment

Based on the probability distribution of wind speed and wind direction, the next step is to calculate the alternating stress of the conductor under different wind speed and wind direction conditions. Since fatigue of the conductor is a fatigue problem under asymmetric, fully reversed alternating stress, especially as dynamic bending strain controls the main factor of fatigue failure, the static stress of the outer aluminum strands also affects the fatigue life. In this case, the Goodman linear method is widely used to calculate the equivalent alternating stress of the stress amplitude. The Goodman linear method is based on the interaction between the static stress and

alternating stress of the material. By establishing the equivalent relationship between static stress and alternating stress, asymmetric stress is converted into an equivalent alternating stress. Let the equivalent alternating stress value be represented by δ_{rw} , the dynamic bending stress value of mild wind vibration be represented by δ_z , the ultimate strength of the conductor be represented by δ_y , and the static stress value of the conductor be represented by δ_l . The Goodman linear method defines the equivalent alternating stress formula as:

$$\frac{\delta_z}{\delta_{rw}} + \frac{\delta_l}{\delta_y} = 1 \quad (10)$$

Once the stress amplitude of the conductor is calculated, the fatigue damage can be assessed using Miner's cumulative damage theory. According to the method recommended by the CIGRE 22nd Committee, Working Group 04, the Miner cumulative damage theory is widely used for estimating the fatigue life of conductors. Under each wind speed and wind direction condition, the conductor experiences alternating stresses of different amplitudes, which cause microscopic damage to the material. According to Miner's theory, the accumulation of fatigue damage is linear, and the total damage rate can be estimated by summing the damage under different stress conditions. Let the damage rate of the material under the u -th stress condition be defined as F_u . When the stress change $\Delta\delta_u$ occurs, the number of vibrations is represented by $v(\Delta\delta_u)$, and the number of conductor failures is represented by $V(\Delta\delta_u)$. The total damage rate F can be calculated using the following formula:

$$F = \sum_u F_u = \sum_u \frac{v(\Delta\delta_u)}{V(\Delta\delta_u)} \quad (11)$$

δ can be obtained using the Wöhler safety curve fitting formula:

$$\delta = \begin{cases} 450V^{-0.2} & V \leq 2 \times 10^7 \\ 263V^{-0.168} & V > 2 \times 10^7 \end{cases} \quad (12)$$

Through thermo-mechanical coupling analysis, it is found that under conditions of large day-night temperature differences, the temperature distribution of the conductor undergoes periodic changes, resulting in fluctuations in the material's thermal stress. These temperature changes significantly affect the conductor's stress state and fatigue life. In this process, the temperature field and stress field of the conductor need to be analyzed synchronously. By correcting the fatigue strength curve and considering the temperature correction on fatigue life, a more accurate fatigue life prediction can be obtained. Let the wind direction frequency be represented by O_{df} , and the correction factor by Ω . The fatigue life of the high voltage transmission conductor is given by:

$$X = \frac{\Omega O_{df}}{F} \quad (13)$$

After completing the above steps, the final fatigue life estimation can be derived through the following key steps:

Step 1: Calculate the amplitude of micro-wind vibration and dynamic bending strain of the conductor

In a high-temperature, high-humidity environment, the conductor is subjected to micro-wind forces, causing periodic micro-vibrations. Due to temperature and humidity changes in the environment, the amplitude of these micro-wind vibrations may fluctuate. Therefore, this paper uses the energy balance method to determine the amplitude of the micro-wind vibration of the conductor. By performing an energy balance analysis on the conductor's vibration energy, the vibration amplitude of the conductor under wind speed can be accurately calculated. Further, the dynamic bending strain δ_z of the conductor is calculated. Dynamic bending strain is a major factor affecting the conductor's fatigue failure, especially under alternating stress, as it significantly impacts the material's fatigue life. Based on the structural characteristics and vibration amplitude of the conductor, the dynamic bending strain is calculated using the corresponding formula. Next, using the equivalent stress alternating formula, the dynamic bending strain is converted into the equivalent alternating stress δ_{rw} . This process is corrected and transformed using Goodman's linear method, considering the combined effect of static and alternating stresses. The obtained equivalent alternating stress δ_{rw} will be used for subsequent fatigue life analysis.

Step 2: Calculate fatigue life based on the S-N curve

Once the equivalent alternating stress δ_{rw} is obtained, the next step is to use the S-N curve to determine the number of vibrations V required for fatigue failure at this stress level. The S-N curve is typically obtained experimentally and describes the fatigue life of materials under different stress amplitudes. In high-temperature, high-humidity environments, the fatigue limit of the S-N curve may change, so the effects of temperature and humidity on material fatigue performance need to be considered. Specifically, high temperatures usually lead to a decrease in the fatigue limit, so the S-N curve should be appropriately corrected to obtain the actual fatigue life under these environmental conditions. Using the S-N curve, combined with the value of equivalent alternating stress δ_{rw} , the corresponding number of vibrations V can be determined, which represents the maximum number of vibrations the conductor can withstand under this stress condition.

Step 3: Calculate the number of vibrations based on wind speed and wind direction probability distributions

Since wind speed and wind direction in the conductor's environment will vary, it is necessary to calculate the number of vibrations that occur at the equivalent alternating stress δ_{rw} level based on the actual wind speed and wind direction probability distributions. Specifically, changes in wind speed and wind direction determine the frequency and amplitude of the conductor's vibrations. In high-temperature, high-humidity environments, wind speed may be affected by seasonal changes, so the probability distributions of wind speed and wind direction need to be modeled based on historical meteorological data, with appropriate statistical methods used for fitting. By using the probability distributions of wind speed and wind direction, the actual number of vibrations δ_{rw} that occur at the equivalent alternating stress δ_{rw} level can be calculated. This number reflects the frequency of the micro-wind vibrations experienced by the conductor under specific environmental conditions, and serves as the foundational data for calculating fatigue damage.

Step 4: Calculate total damage rate based on Miner's cumulative damage theory

With the number of vibrations V corresponding to the equivalent alternating stress δ_{rw} and the actual number of vibrations δ_{rw} , the total damage rate F of the conductor can then be calculated using Miner's cumulative damage theory. According to Miner's theory, fatigue damage is cumulative, and the damage rates under different stress levels are linearly additive.

Step 5: Consider the impact of high temperature and high humidity on fatigue life

In a high-temperature, high-humidity environment, the material properties of the conductor will undergo certain changes, especially the fatigue limit and mechanical properties of aluminum alloy materials, which are affected by temperature and humidity. Therefore, when calculating fatigue life, the S-N curve should be corrected for temperature and humidity. High temperatures lead to a decrease in the material's yield strength, which reduces the fatigue life, while high humidity may accelerate material corrosion, further affecting the fatigue life.

4. EXPERIMENTAL RESULTS AND ANALYSIS

According to the experimental data shown in Table 1, the changes in temperature and humidity have a significant impact on both the theoretical and calculated values of vertical thermal stress in each layer of the high-voltage transmission line. As the temperature increases from 30°C to 70°C and the humidity increases from 40% to 80%, the thermal stress levels in each layer of the conductor increase overall. For example, in the steel core layer and the 1st layer of the aluminum strand, when the temperature is 30°C and humidity is 40%, the theoretical value of the steel core layer is 211.54 N/mm² and the calculated value is 213.26 N/mm². However, when the temperature is 70°C and humidity is 80%, the theoretical value of the steel core layer rises to 256.31 N/mm², and the calculated value is 256.36 N/mm². A similar trend is observed in the 1st and 2nd layers of the aluminum strand, where the increase in temperature and humidity causes the stress values to rise. For instance, at 30°C and 40% humidity, the theoretical value of the 1st layer of the aluminum strand is 48.56 N/mm² and the calculated value is 51.23 N/mm². At 70°C and 80% humidity, the theoretical value of the 1st layer is 48.26 N/mm² and the calculated value is 48.23 N/mm². By analyzing the data in Table 1, it is evident that in high-temperature and high-humidity environmental conditions, the thermal stress of the conductor shows a significant increasing trend. This is mainly due to the increased thermal expansion of the material as the temperature rises, while the increase in humidity may cause some of the material's physical properties to change, further intensifying the accumulation of thermal stress. The stress variation in the steel core layer is more pronounced than that in the aluminum strand layer, indicating that the thermal expansion of the steel core material is more sensitive to temperature and humidity changes. Especially under high temperature and high humidity conditions, the vertical thermal stresses in both the steel core and aluminum strand layers are close to their limit values, meaning that the conductor's load-bearing capacity and stability may be threatened at this point.

According to the data shown in Table 2, temperature changes have a significant effect on the thermal stress of each layer of strands in the high-voltage transmission line. Under conditions of 30°C and 40% humidity, the thermal stress of the 1st layer of the steel core layer is 256.32 MPa and 258.69 MPa

for the 2nd layer, while the 1st layer of the aluminum strand is 48.26 MPa and the 2nd layer is 46.25 MPa. As the temperature gradually increases to 40°C, 50°C, 60°C, and 70°C, the thermal stress in the steel core layer shows a downward trend, with the 1st and 2nd layers decreasing from 248.29 MPa to 223.58 MPa and from 258.69 MPa to 223.26 MPa, respectively. The aluminum strand layer exhibits a different trend. The thermal stress in the 1st layer decreases to 46.51 MPa at 40°C but then increases at higher temperatures, reaching 42.69 MPa at 70°C. The thermal stress of the 2nd layer increases progressively with the rise in temperature, from 46.25 MPa to 61.28 MPa. It can be seen that under fixed humidity (40%), the thermal stress in the steel core layer significantly decreases as the temperature increases, while the thermal stress in the aluminum strand layer shows a relatively complex change trend, especially for the 2nd layer, where thermal stress gradually increases under high-temperature conditions. By analyzing the data in Table 2, it can be concluded that the increase in temperature has varying degrees of impact on the thermal stress in the different layers of the high-voltage transmission line. In the steel core layer, as the temperature increases, the thermal stress decreases overall, indicating that the material in the steel core layer undergoes significant thermal expansion under high-temperature conditions, which reduces its internal stress. The aluminum strand layer exhibits different thermal stress changes, especially for the 2nd layer, where the thermal stress increases with temperature. This may be related to the yield characteristics and thermal expansion behavior of aluminum at high temperatures. In high-

temperature environments, the increase in thermal stress in the aluminum strand layer may lead to a reduction in its fatigue life. Combining the thermodynamic model analysis results in this paper, it can be inferred that the increase in temperature will increase the stress distribution difference in the conductor material, which may intensify fatigue damage in high-temperature environments. Therefore, under high-temperature and high-humidity conditions, it is necessary to consider the fatigue performance of the conductor material and the impact of temperature and humidity on its long-term stability.

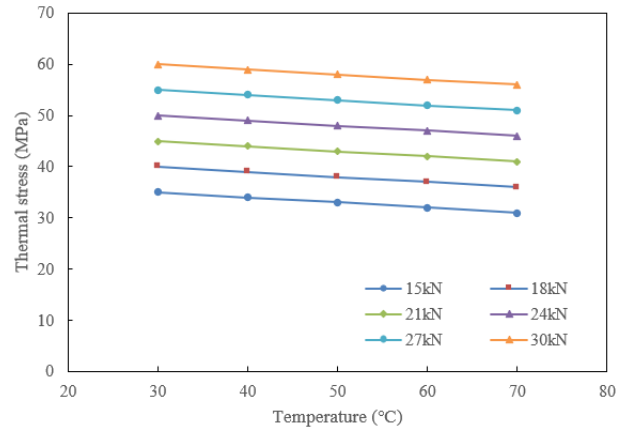


Figure 5. Relationship between thermal stress value of the outer strand of high-voltage transmission line and conductor temperature under different tension forces

Table 1. Vertical thermal stress of high-voltage transmission lines in different layers under various temperature and humidity conditions

Environmental Conditions	Vertical Stress	Steel Core Layer		Aluminum Strand Layer	
		1st Layer	2nd Layer	1st Layer	2nd Layer
Temperature 30°C/Humidity 40%	Theoretical Value	211.54	198.54	48.56	46.25
	Calculated Value	213.26	214.21	51.23	52.12
Temperature 40°C/Humidity 50%	Theoretical Value	224.20	223.56	47.62	44.26
	Calculated Value	226.36	224.10	52.31	48.23
Temperature 50°C/Humidity 60%	Theoretical Value	224.58	225.26	47.95	45.23
	Calculated Value	223.32	224.78	51.23	47.23
Temperature 60°C/Humidity 70%	Theoretical Value	245.85	236.98	47.62	43.21
	Calculated Value	246.28	235.59	48.26	47.26
Temperature 70°C/Humidity 80%	Theoretical Value	256.31	256.21	48.26	43.26
	Calculated Value	256.36	259.85	48.23	46.25

Table 2. Thermal stress values of each layer of strands of high-voltage transmission line under fixed humidity and different temperature conditions

Environmental Conditions	Steel Core Layer (MPa)		Aluminum Strand Layer (MPa)	
	1st Layer	2nd Layer	1st Layer	2nd Layer
Temperature 30°C/Humidity 40%	256.32	258.69	48.26	46.25
Temperature 40°C/Humidity 40%	248.29	246.31	46.51	51.23
Temperature 50°C/Humidity 40%	246.23	236.25	44.23	52.36
Temperature 60°C/Humidity 40%	236.25	223.56	42.23	55.36
Temperature 70°C/Humidity 40%	223.58	223.26	42.69	61.28

Table 3. Heat stress values of each layer of strands in high voltage transmission conductor under different humidity conditions at fixed temperature

Environmental Conditions	Steel Core Layer (MPa)		Aluminum Strand Layer (MPa)	
	1st Layer	2nd Layer	1st Layer	2nd Layer
Temperature 30°C/Humidity 40%	245.36	239.56	48.52	47.56
Temperature 30°C/Humidity 50%	239.58	235.5	46.25	52.32
Temperature 30°C/Humidity 60%	223.65	224.23	44.23	53.23
Temperature 30°C/Humidity 70%	224.56	226.23	42.31	56.24
Temperature 30°C/Humidity 80%	235.23	223.32	42.36	62.36

Table 4. Vibration counts at different frequencies considering the temperature of high voltage transmission conductor

Frequency (Hz)	Vibration Count ($\times 10^7$)	Vibration Amplitude (mm)	Strand Heat Stress (MPa)	Equivalent Alternating Stress (MPa)	S-N Curve Vibration Count ($\times 10^7$)
13	1.5325	23.23	32.35	17.26	0.88
18	2.8956	45.26	26.23	16.23	1.23
23	1.4852	9.21	21.26	11.26	8.45
28	6.1235	5.46	18.23	9.26	43.23
33	7.4526	3.23	14.26	6.32	512.32
38	8.7546	2.45	12.32	4.26	2451.23
43	9.5623	1.36	12.36	3.26	8895.36
48	11.2352	1.12	11.25	3.21	27851.23
53	12.2355	0.82	13.26	2.23	77892.23
58	11.2468	0.63	11.58	2.15	223254.26

According to the data in Figure 5, the thermal stress value of the outer strand of the high-voltage transmission line shows a regular change with the temperature under different tension forces. When the applied tension is 15 kN, as the temperature increases from 30°C to 70°C, the thermal stress value of the outer strand decreases from 35 N/mm² to 31 N/mm². Under 18 kN tension, the change in thermal stress is relatively stable, with the thermal stress value of the outer strand decreasing from 40 N/mm² to 36 N/mm² as the temperature increases from 30°C to 70°C. For 21 kN and 24 kN tension, the decrease in thermal stress value is smaller, decreasing from 45 N/mm² to 41 N/mm² and from 50 N/mm² to 46 N/mm², respectively. Finally, under the maximum tension of 27 kN, the change in the thermal stress value of the outer strand is the smallest, showing a decrease from 55 N/mm² to 51 N/mm². By analyzing the data in the figure, it can be observed that as the temperature increases, the thermal stress value of the outer strand generally shows a downward trend. This phenomenon indicates that under high-temperature conditions, the thermal expansion of the outer strand causes the conductor to elongate, thereby reducing the thermal stress experienced by the material. Under different tension forces, the degree of change in thermal stress varies. The higher the tension, the smaller the decrease in thermal stress. This is because higher applied tension can effectively limit the thermal expansion of the conductor, leading to a more gradual reduction in thermal stress.

According to the data in Table 3, at a fixed temperature of 30°C, as humidity increases, the heat stress of each layer of strands in the high voltage transmission conductor shows significant changes. For the steel core layer, the heat stress of the 1st layer gradually decreases from 245.36 MPa at 40% humidity to 235.23 MPa at 80% humidity, and the 2nd layer decreases from 239.56 MPa to 223.32 MPa. The aluminum strands layer shows a different trend. The heat stress of the 1st layer decreases gradually from 48.52 MPa at 40% humidity to 42.31 MPa at 70% humidity but shows a slight rebound to 42.36 MPa at 80% humidity. The 2nd layer's heat stress increases significantly, rising from 47.56 MPa at 40% humidity to 62.36 MPa at 80% humidity, showing a clear upward trend. From the experimental data in Table 3, it is evident that humidity has a significant impact on the heat stress of the high voltage transmission conductor. For the steel core layer, as humidity increases, heat stress gradually decreases, possibly because higher humidity may affect the material's thermal expansion characteristics due to water absorption inside the material, thus reducing heat stress. However, the heat stress in the aluminum strands layer exhibits a more complex change. The heat stress of the 1st layer decreases as humidity increases, indicating that the

thermal expansion characteristics of aluminum are relatively stable under increasing humidity. But when humidity further increases, there is a rebound, which may be related to the impact of humidity on the microscopic structure of the aluminum strands material and its synergistic effect with the steel core layer. The heat stress in the 2nd layer of the aluminum strands increases significantly with rising humidity, indicating that humidity has a more significant effect on the aluminum strands, potentially enhancing the expansion force and thus increasing the internal stress.

The data in Table 4 shows that at different frequencies, as the vibration count increases, the strand heat stress and equivalent alternating stress of the high voltage transmission conductor exhibit a certain regular variation. Specifically, at low frequencies (e.g., 1.53 Hz), the vibration count is 23.23×10^7 , the strand heat stress is 32.35 MPa, and the equivalent alternating stress is 17.26 MPa. As the frequency increases, the vibration count and amplitude gradually increase, and the strand heat stress also changes. For instance, at a frequency of 12.23 Hz, the vibration count reaches 223254×10^7 , the strand heat stress reaches 12.36 MPa, and the equivalent alternating stress is 2.23 MPa. From the changes in vibration count, it is evident that higher frequencies correspond to significantly increased vibration counts, the strand heat stress gradually decreases, and the equivalent alternating stress tends to be lower at higher frequencies. Overall, there is an inverse relationship between vibration frequency and strand heat stress, and the equivalent alternating stress decreases as the vibration count increases. From the data analysis in Table 4, it can be concluded that vibration frequency has an important impact on the strand heat stress and equivalent alternating stress of high voltage transmission conductors. At lower frequencies, the conductor's heat stress is higher, while at higher frequencies, the heat stress is relatively lower, indicating that the higher the frequency, the weaker the stress response caused by thermal expansion and vibration of the conductor. This phenomenon can be explained from a fatigue performance perspective: as the frequency increases, the vibration cycle shortens, and the stress changes more rapidly in each cycle, which may lead to stress relief inside the material and thus reduce the accumulation of fatigue damage.

From the fatigue life data in Figure 6, it can be inferred that the conductor temperature has a very complex effect on its fatigue life, with certain nonlinear characteristics. Generally, temperature has a direct impact on the material's fatigue life, especially at high temperatures, where the material's strength, hardness, and other physical properties may change, thus affecting the accumulation of fatigue damage and life prediction. The data in the table show that as the temperature increases, the fatigue life of the conductor significantly

increases, possibly due to the change in the conductor material's thermal expansion characteristics at higher temperatures, which alters the distribution of thermal stress. This results in lower alternating stresses experienced by the conductor material during long-term operation, thereby slowing down the fatigue damage process. Although high temperatures may induce more thermal stress, the physical properties of the material at high temperatures could lead to a change in the fatigue damage mechanism, ultimately resulting in a longer service life. When designing high-voltage transmission conductors, it is essential to consider the effect of temperature on conductor fatigue life, particularly in high-temperature environments, where material selection and thermal stress analysis should be strengthened to ensure the long-term stability and safety of the conductor.

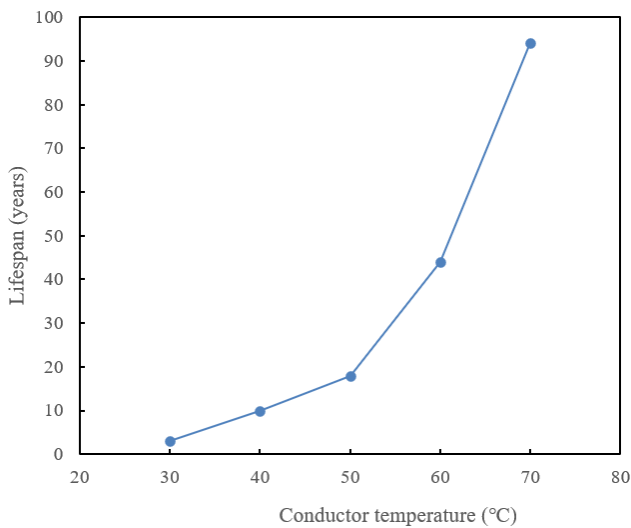


Figure 6. Relationship between conductor fatigue life and conductor temperature

5. CONCLUSION

The main research content of this paper can be divided into two parts: the first part focuses on the calculation and analysis of the thermal stress of high-voltage transmission conductors under high-temperature and high-humidity environments, with an emphasis on the thermal expansion behavior of the conductor and its impact on thermal stress under different temperature and humidity conditions. By establishing a thermodynamic model, this paper accurately describes the thermal expansion and thermal stress of conductors in high-temperature and high-humidity environments, revealing the impact of temperature and humidity variations on conductor thermal stress. The second part, based on the previous thermodynamic analysis, combines the fatigue performance of materials to construct a fatigue life prediction model for high-voltage transmission conductors under high-temperature and high-humidity conditions, providing theoretical support and methodological basis for practical applications. The research results of this paper have important practical value for the design and use of high-voltage transmission conductors under high-temperature and high-humidity environments. Through accurate thermodynamic model analysis, this paper reveals the significant impact of temperature and humidity on conductor thermal expansion and thermal stress, further explaining how these factors, by affecting material fatigue performance,

ultimately determine the conductor's fatigue life. The research shows that temperature and humidity have complex interactions on the conductor's thermal stress and fatigue life. Under high-humidity and high-temperature conditions, conductor thermal stress increases, while the material's fatigue life may be extended due to the change in stress distribution. Furthermore, the fatigue life prediction model in this paper can provide an effective tool for engineering practice to assess the long-term stability and safety of conductors under different environmental conditions.

However, this paper also has certain limitations. First, the study mainly relies on thermodynamic models and experimental data of materials. The model assumptions and experimental conditions may differ from actual application scenarios, especially under extreme weather conditions, which may yield different results. Second, although this paper considers the impact of high temperature and humidity on conductor fatigue life, the analysis does not fully take into account complex factors such as the periodic changes in temperature and humidity and the vibration of conductors during actual operation. Therefore, future research can be extended in the following directions: (1) further optimizing the thermodynamic model to consider more complex environmental factors such as wind speed and climate change; (2) verifying the accuracy and reliability of the model through large-scale field test data; (3) exploring the fatigue performance of different materials under extreme temperature and humidity conditions, aiming to improve the conductor material selection and design standards, and enhance the conductor's stability and durability under variable climate conditions.

REFERENCES

- [1] Halilčević, S.S., Softić, I. (2016). The line and node voltage stability index presented through the porosity of high-voltage transmission lines. *Electric Power Components and Systems*, 44(16): 1865-1876. <https://doi.org/10.1080/15325008.2016.1198436>
- [2] Sadiq, E.H., Mohammed, L.A., Taha, H.M. (2024). Enhancing power transmission efficiency using static synchronous series compensators: A comprehensive review. *Journal of Intelligent Systems and Control*, 3(2): 71-83. <https://doi.org/10.56578/jisc030201>
- [3] Ngo, V.D., Le, D.D., Le, K.H., Pham, V.K., Berizzi, A. (2017). A methodology for determining permissible operating region of power systems according to conditions of static stability limit. *Energies*, 10(8): 1163. <https://doi.org/10.3390/en10081163>
- [4] Anand, M., Chatterjee, D., Goswami, S.K. (2024). Loss minimization based optimal frequency selection for low frequency transmission lines using telegrapher's method. *COMPEL-The International Journal for Computation and Mathematics in Electrical and Electronic Engineering*, 43(1): 121-136. <https://doi.org/10.1108/COMPEL-05-2023-0194>
- [5] Al-Tak, M.A., Ain, M.F.B., Al-Yozbaky, O.S., Jamil, M.K.M. (2024). Sensorless ANFIS-based control of PV-powered double stator induction motors for EVs. *Journal Européen des Systèmes Automatisés*, 57(1): 167-175. <https://doi.org/10.18280/jesa.570117>
- [6] Choi, D., Lee, S.H., Son, G.T., Park, J.W., Baek, S.M. (2018). Planning of HVDC system applied to Korea

- electric power grid. *Journal of Electrical Engineering and Technology*, 13(1): 105-113. <https://doi.org/10.5370/JEET.2018.13.1.105>
- [7] Majstrovic, M., Sutlovic, E., Ramljak, I. (2017). Critical diameter of particles produced in overhead line conductor clashing. *Applied Thermal Engineering*, 114: 713-718. <https://doi.org/10.1016/j.applthermaleng.2016.12.008>
- [8] Savadjiev, K., Farzaneh, M. (2004). Modeling of icing and ice shedding on overhead power lines based on statistical analysis of meteorological data. *IEEE Transactions on Power Delivery*, 19(2): 715-721. <https://doi.org/10.1109/TPWRD.2003.822527>
- [9] Faggian, P., Trevisiol, A., Decimi, G. (2024). Future projections of wet snow frequency and wet snow load on overhead high voltage conductors over Italy. *Cold Regions Science and Technology*, 217: 103980. <https://doi.org/10.1016/j.coldregions.2023.103980>
- [10] Ruszczak, B., Tomaszewski, M. (2014). Extreme value analysis of wet snow loads on power lines. *IEEE Transactions on Power Systems*, 30(1): 457-462. <https://doi.org/10.1109/TPWRS.2014.2321008>
- [11] Shi, H.L., Xiong, B., Huang, K.J., Ding, Y.W., Gu, G.B. (2023). Thermal circuit analysis and performance evaluation of evaporative cooling transformers within advanced industrial logistics infrastructure. *International Journal of Heat and Technology*, 41(3): 498-512. <https://doi.org/10.18280/ijht.410303>
- [12] Tomaszewski, M. (2012). Measurement of wet snow loads on overhead power line conductors. *PRZEGLAD ELEKTROTECHNICZNY*, 88(10 B): 21-23.
- [13] Tomaszewski, M., Ruszczak, B. (2013). Analysis of frequency of occurrence of weather conditions favouring wet snow adhesion and accretion on overhead power lines in Poland. *Cold Regions Science and Technology*, 85: 102-108. <https://doi.org/10.1016/j.coldregions.2012.08.007>
- [14] Yao, H.W., Lv, K.F., Yan, S.K., Xing, M.Y., Lou, Z., Ren, W. (2023). Simulation study on fire combustion process of oil immersed transformer. *International Journal of Heat and Technology*, 41(2): 455-461. <https://doi.org/10.18280/ijht.410221>
- [15] Božiček, A., Franc, B., Filipović-Grčić, B. (2022). Early warning weather hazard system for power system control. *Energies*, 15(6): 2085. <https://doi.org/10.3390/en15062085>
- [16] Bayani, R., Waseem, M., Manshadi, S.D., Davani, H. (2022). Quantifying the risk of wildfire ignition by power lines under extreme weather conditions. *IEEE Systems Journal*, 17(1): 1024-1034. <https://doi.org/10.1109/JSYST.2022.3188300>
- [17] Liu, Y., Lei, S., Hou, Y. (2019). Overhead transmission line outage rate estimation under wind storms. *IEEE Transactions on Electrical and Electronic Engineering*, 14(1): 57-66. <https://doi.org/10.1002/tee.22765>
- [18] Sterc, T., Filipovic-Grbic, B., Franc, B., Mesic, K. (2023). Methods for estimation of OHL conductor temperature based on ANN and regression analysis. *International Journal of Electrical Power & Energy Systems*, 151: 109192. <https://doi.org/10.1016/j.ijepes.2023.109192>
- [19] Gonçalves, A., Marques, M.C., Loureiro, S., Nieto, R., Liberato, M.L. (2023). Disruption risk analysis of the overhead power lines in Portugal. *Energy*, 263: 125583. <https://doi.org/10.1016/j.energy.2022.125583>
- [20] Wang, J., Xiong, X., Li, Z., Wang, W., Zhu, J. (2016). Wind forecast-based probabilistic early warning method of wind swing discharge for OHTLs. *IEEE Transactions on Power Delivery*, 31(5): 2169-2178. <https://doi.org/10.1109/TPWRD.2016.2519599>
- [21] Yin, W., Feng, S., Hou, J., Qian, C., Hou, Y. (2022). A decision-dependent stochastic approach for joint operation and maintenance of overhead transmission lines after sandstorms. *IEEE Systems Journal*, 17(1): 1489-1500. <https://doi.org/10.1109/JSYST.2022.3185072>
- [22] Mahin, A.U., Islam, S.N., Ahmed, F., Hossain, M.F. (2022). Measurement and monitoring of overhead transmission line sag in smart grid: A review. *IET Generation, Transmission & Distribution*, 16(1): 1-18. <https://doi.org/10.1049/gtd2.12271>
- [23] Billinton, R., Acharya, J.R. (2006). Weather-based distribution system reliability evaluation. *IEE Proceedings-Generation, Transmission and Distribution*, 153(5): 499-506. <https://doi.org/10.1049/ip-gtd:20050427>